

# Rheology and Relaxation Processes in a Melting Thermotropic Liquid–Crystalline Polymer

Ruobing Yu,<sup>1</sup> Wei Yu,<sup>2</sup> Chixing Zhou,<sup>2</sup> J. J. Feng<sup>3,4</sup>

<sup>1</sup>School of Materials Science and Engineering, East China University of Science and Technology, Shanghai 200237, China

<sup>2</sup>Department of Polymer Science and Engineering, Shanghai Jiao Tong University, Shanghai 200240, China

<sup>3</sup>Department of Chemical and Biological Engineering, University of British Columbia, Vancouver, BC V6T 1Z4, Canada

<sup>4</sup>Department of Mathematics, University of British Columbia, Vancouver, BC V6T 1Z4, Canada

Received 18 April 2006; accepted 19 September 2006

DOI 10.1002/app.25953

Published online in Wiley InterScience (www.interscience.wiley.com).

**ABSTRACT:** The relaxation behavior of a thermotropic liquid–crystalline polymer (TLCP), LC-5000 from Unichika, Japan, was investigated by rheology and optical microscopy. The solid–nematic transition was shown by DSC and dynamic temperature ramp. The transitions of dynamic modulus with temperature correspond to the end of the melting process. The TLCP is composed of unmelted solid crystals and nematic liquid crystal during the melting process. Macroscopically, it changes from a viscoelastic solid to a viscoelastic liquid in this process, as verified by creep test and dynamic frequency sweep under different temperature. The relaxation spectra of

the TLCP under different temperature were calculated from the dynamic modulus. The characteristic relaxation processes determined from the relaxation spectrum are consistent with the observation from polarized optical microscopy. During melting, in particular, the relaxation of deformed polydomains and chain orientation slows down due to the constraining effects of unmelted solid crystals. © 2007 Wiley Periodicals, Inc. *J Appl Polym Sci* 104: 3780–3787, 2007

**Key words:** liquid–crystalline polymer; rheology; relaxation

## INTRODUCTION

Thermotropic liquid–crystalline polymers (TLCPs) have been the subject of many studies due to their intrinsically anisotropic structure. These ordered structures and the proliferation of defects lead to unusual rheological behavior such as a negative first normal stress difference and thermal history effects.<sup>1</sup> Moreover, the relaxation behaviors of TLCPs are much more complicated than those of flexible polymers due to the presence of polydomain structure, whose equilibrium state is hard to define. Numerous investigations have been made on the rheological properties and relaxation behavior of TLCPs in nematic state.<sup>1–18</sup>

Wissburn<sup>8</sup> points out that liquid–crystalline polymers typically possess long relaxation times, up to 100 times longer than those of isotropic polymers of

similar molecular weight. Step strain experiments show a fast initial stress relaxation followed by a slower relaxation period, and a tail in the relaxation curve is observed, which has led to the speculation that some structure or unmelted solid phase exists.<sup>9</sup> Amundson et al.<sup>10</sup> have used proton and C<sup>13</sup> NMR to study the microstructure of the HBA/PET(80/20) polymer (provided by Tennessee Eastman). Some results<sup>10–11</sup> show that the HBA/PET(80/20) polymer (provided by Tennessee Eastman) is a three-phase system at melt temperature (a nematic melt phase, a crystalline homopolymer phase, and a nonlayered periodic crystal), that is to say, at melt temperature, there is a mixture of nematic liquid crystal and solid. The shear and normal stress after cessation of flow also show a fast initial relaxation followed by a long tail.<sup>12–15</sup> Langelaan and Gotsis<sup>12</sup> concluded that the fast initial decay is independent of the previous shear rate and is ascribed to local molecular rearrangements, while the second part of the relaxation involves the director profile. Lee and Han<sup>16</sup> found that the relaxation rate of shear stress is slower as the applied shear rate during shear flow is increased. Wiberg et al.<sup>17</sup> assess the relaxation of orientation in a sheared thermotropic liquid–crystalline copolyester by means of transmitted light intensity through crossed polarizers in a shear cell. They observe that the relaxation of orientation is very short. A notable

Correspondence to: C. Zhou (cxzhou@sjtu.edu.cn).

Contract grant sponsor: National Natural Science Foundation of China; contract grant numbers: 20174024, 20204007, and 50290090.

Contract grant sponsor: US National Science Foundation; contract grant numbers: CTS-9984402, CTS-0229298.

*Journal of Applied Polymer Science*, Vol. 104, 3780–3787 (2007)  
© 2007 Wiley Periodicals, Inc.

morphological feature is the banded structure after cessation of shear, with parallel bands perpendicular to the shear flow direction. The bands are believed to be associated with a relaxation process.<sup>18–20</sup>

Most previous studies have focused on the rheology and relaxation of a TLCP in fully nematic state. However, Tormes et al.<sup>21</sup> studied rheology of Rodrum 5000 at 290°C (above melting temperature), which shows characteristics of a viscoelastic solid. This was attributed to a three-dimensional network on the basis of a collection of small monodomains, which gave rise to a threaded texture. It was found that  $G'$ ,  $G''$ , and  $\eta^*$  of Rodrum 5000 at 290°C in dynamic time sweep grew in a concave way, which was demonstrated by the growth of high melting temperature crystallites.

Because of the complex structure of TLCPs, they typically have a wide melting range. In fact, they may not be in a complete nematic phase above the nominal melting temperature. In the melting process, a TLCP will become a mixture of nematic liquid crystal and unmelted solid crystals.<sup>22</sup> Because of the existence of solid crystals in the melting process, the rheology and relaxation behavior of a TLCP would be different from those in pure nematic state. The relaxation dynamics in the transition regime from solid crystals to a nematic liquid crystal have not been investigated thoroughly, and are expected to be quite complex. This study strives to shed some new light on the relaxation behavior of a TLCP during melting by rheological measurements and optical microscopy.

## EXPERIMENTAL

### Materials

The TLCP used here is LC-5000 from Unichika (Inoue, Japan), which is a copolymer of 80-mol % *para*-hydroxybenzoic acid and 20% poly(ethylene terephthalate). This material has a more random monomer sequence than Eastman Kodak's copolyester. As-received pellets of LC-5000 were dried at 180°C under nitrogen for 4 h and kept under vacuum at 90°C before use.

### Rheological measurements

The rheological experiments were performed on a Haake RheoStress 300 with parallel plates of diameter 20 mm and a gap of 1 mm. Dynamic and creep experiments were done to investigate the rheological properties of LC-5000. Dynamic strain sweep was done at 1 Hz in the strain-controlled mode. Dynamic frequency sweep was performed at constant strain in the strain-controlled mode. Dynamic temperature ramp was performed at frequency of 2 Hz, from 270

to 340°C, with the heating rate of 1°C/min. Dynamic frequency sweep was done under different temperature (280, 285, 290, and 295°C) with a strain amplitude of 5%, which is chosen to ensure all the dynamic experiments to be in the linear viscoelastic regime. Creep tests were performed by the application of constant stress 1 Pa for at least 1000 s.

### Optical microscopy

The textures of melting LC-5000 and the evolution of the textures of LC-5000 after a step shear strain, applied by a glass slide over the melting LC-5000, were observed by using optical microscopy (POM) (Leica, Wetzlar, Germany) with hot stage under crossed polarizers.

### Differential scanning calorimeter

The melting of LC-5000 was investigated by using Perkin–Elmer Pyris-1 differential scanning calorimeter (DSC). The sample was heated from room temperature to 340°C at a rate of 20°C/min. This first scan was used to determine the thermal transitions.

## RESULTS AND DISCUSSION

### Melting process

The melting process of LC-5000 is investigated by DSC and dynamic temperature ramp. The DSC thermogram of LC-5000 is shown in Figure 1, which illustrates a melting range from about 270 to 293°C and a nominal melting temperature of 275°C. The melting temperature  $T_m$  determined here is slightly different from that (283°C) reported by Hiseh et al.<sup>23</sup> This is probably due to the different thermal history of the samples, and we did not investigate this

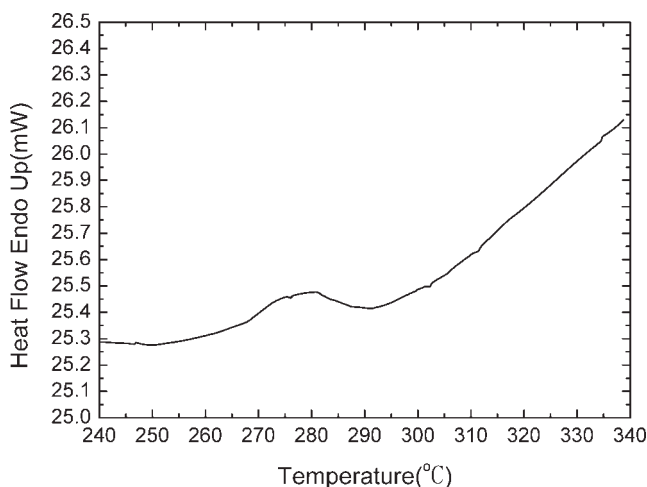


**Figure 1** DSC thermogram of LC-5000 measured at a heating rate of 20°C/min.

discrepancy further. From Figure 1, we can see that the material is fully mesophasic above 293°C. Between 270 and 293°C, LC-5000 is a combination of crystals and liquid crystal (semisolid state). Gao et al.<sup>22</sup> studied phase transition of HBA/HQ/SA copolyester by DSC, which shows that the copolyester is in the crystal/mesophasic biphasic (semisolid state) during the melting range and between complete melting and isotropic transition it appears fully mesophasic.

The results of dynamic temperature ramp are shown in Figure 2. Both  $G'$  and  $G''$  decrease with the increase of temperature, and show a change of slope at about 294–295°C. This transition is more clearly shown in  $\tan \delta$ , which has a peak at about 294°C. This temperature is consistent with the end of the melting process as shown by the DSC. The loss tangent  $\tan \delta$  is believed to be more sensitive to the structure variation than DSC. As the temperature reaches the melting point of certain solid crystals (about 270°C), the TLCP molecules gradually lose

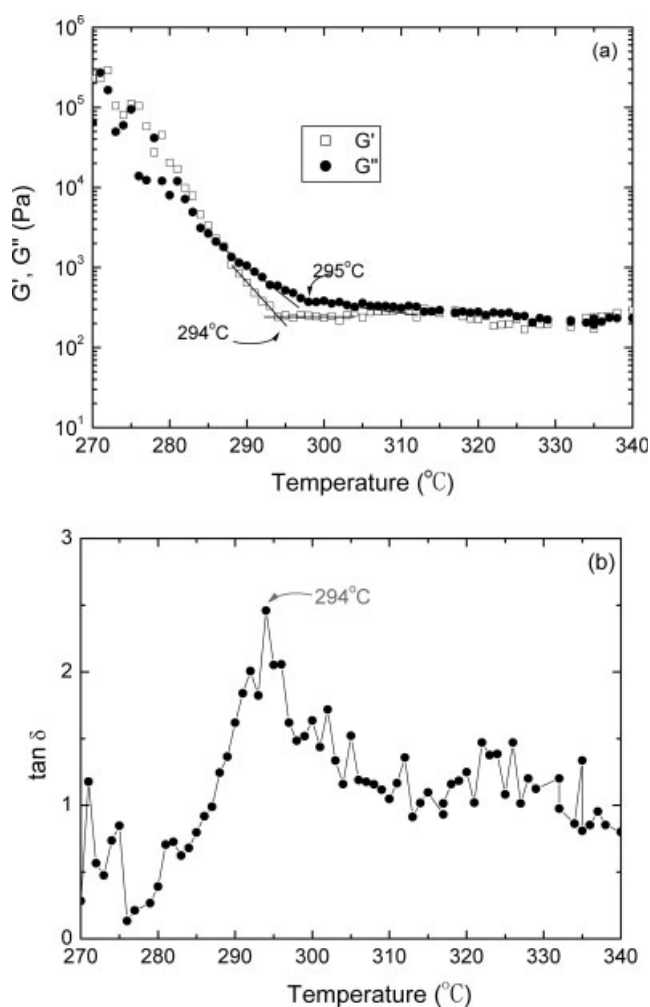


**Figure 2** Dynamic temperature ramp of LC-5000: (a) dynamic modulus; (b)  $\tan \delta$ .

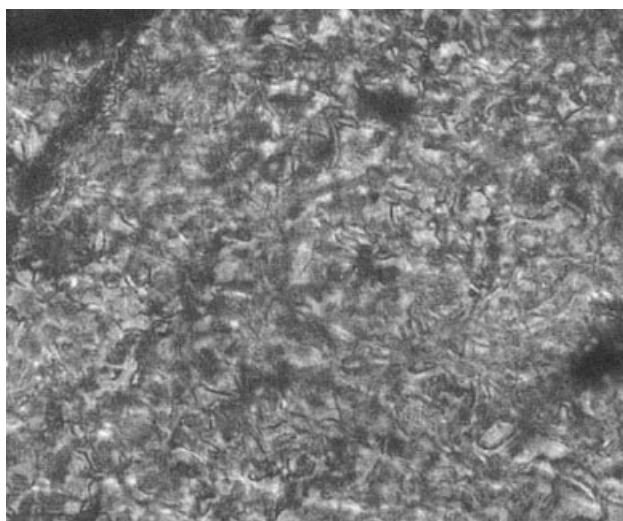


**Figure 3** Micrograph of LC-5000 at 295°C.

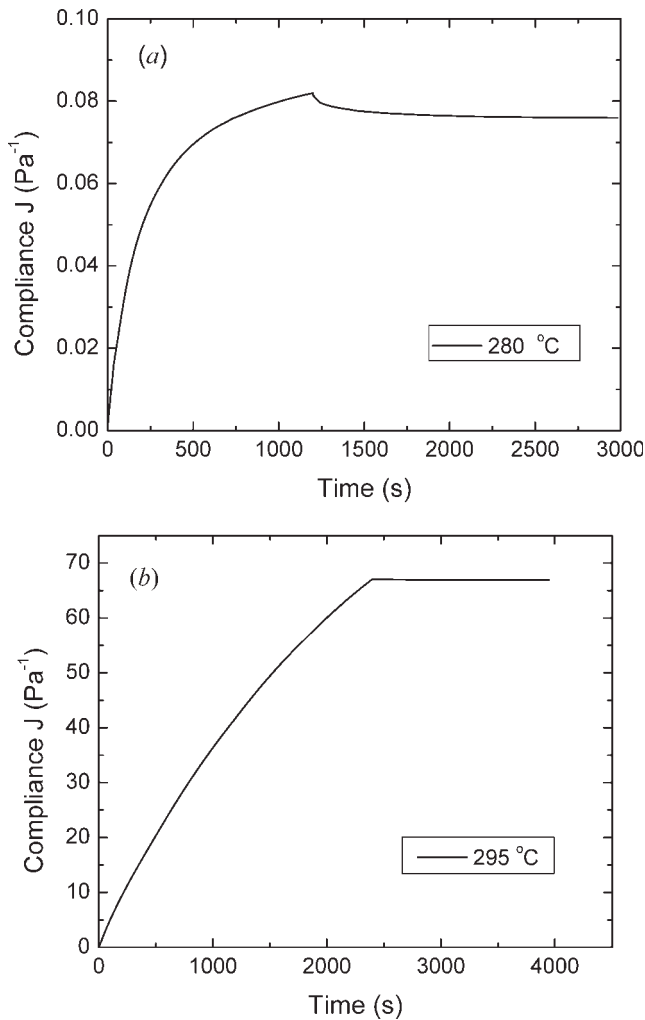
the long-range order of position, but still keep the short-range order of orientation. The sample becomes a mixture of solid crystals and a liquid crystal. The solid crystals gradually disappear as temperature increases further. At the end of melting process (about 294°C), the solid crystals have melted completely and the sample becomes liquid crystal. Therefore, the peak in  $\tan \delta$  represents the transition from solid state to liquid crystal state. One may expect another transition in  $\tan \delta$  at about 270°C showing the start of melting process. However, such a transition is not discerned in the present experiments since the sample is almost solid under 270°C and the data are noisy below this temperature.

Figure 3 shows optical texture of LC-5000 at 295°C. Observation with polarizing optical microscope shows that LC-5000 displays a typical threads texture, characteristic of a nematic state.<sup>21,22</sup> We can conclude that LC-5000 is a pure nematic liquid crystal at the end of melting process.

### Rheological properties and structural change

The compliance of LC-5000 under creep and recovery at 280 and 295°C is shown in Figure 4. LC-5000 exhibits a very small creep compliance ( $<0.1 \text{ Pa}^{-1}$ ) and a compliance plateau appears at 280°C, which is characteristic of solid-like behavior. The creep compliance at 295°C is about three orders of magnitude higher than that at 280°C, and represents a typical liquid-like behavior. This is consistent with the results of DSC and dynamic temperature ramp that the sample at 280°C is a mixture of solid crystals and a liquid crystal, while at 295°C, it is a pure nematic liquid crystal.

The results of dynamic strain sweep (Fig. 5) further reflect the different content of solid crystals in LC-5000



**Figure 4** Compliance of LC-5000 as a function of time (a) at 280°C; (b) at 295°C.

at different temperature. The regime of linear viscoelasticity extends as the temperature increases. This is similar to the behavior of polymer composites whose regime of linear viscoelasticity shrinks as the content of solid particles increases. Correspondingly, we can say that the content of solid crystals decreases as the temperature increases. These results are consistent with the experiments of Tormes et al.,<sup>21</sup> who showed that LC-5000 at 290°C exhibits viscoelastic solid characteristic, and may be considered a suspension of solid particles in a viscous matrix. However, Tormes et al.'s conjecture that the viscoelastic solid characteristic was caused by polydomain structure is not supported by our results. Polydomains are typical structure in nematic LCP, and yet no solid-like behavior is observed for a TLCP in pure nematic state [Fig. 4(b)]. The solid-like behavior of LC-5000 at 290°C as shown by Tormes et al.<sup>21</sup> is probably due to the existence of unmelted solid crystals in the sample.

We know from the rheology of polymer filled with solid particles that the contents of solid particles can

be related to the loss modulus of the composites.<sup>24</sup> For intermediate and high volume content of solid particles, the Maron-Pierce equation gives:

$$G'' = G_m'' \left[ 1 + \left( 0.75 \frac{\phi}{\phi_m} \right) / \left( 1 - \frac{\phi}{\phi_m} \right) \right]^2 \quad (1)$$

where  $G''$  is the loss modulus of the composite of polymer and solid particles,  $G_m''$  is the modulus of the matrix polymer,  $\phi$  is the content of solid particles, and  $\phi_m$  is the geometric percolation volume.  $\phi_m$  can be evaluated for particles with specific shape. However, the exactly shape of solid crystals in LC-5000 is unknown here, and  $\phi_m$  is difficult to estimate. We have used the reduced ratio  $\phi/\phi_m$  to evaluate the relative content of solid crystals. To compare the solid contents under different temperature, we assume that  $\phi_m$  stays the same under different temperature. In its original application,  $G_m''$  denotes the loss modulus of the matrix. In our case, it should be the loss modulus of LC-5000 in the fully nematic state at the temperature. To measure the composite modulus  $G''$ , we first heat the sample to 320°C and anneal it for 5min to ensure complete melting and to eliminate the thermal history (as LC-5000 used by us is more random than Eastman Kodak's copolyester, there are not high-melting crystals. 320°C is enough to make LC-5000 completely melt. At higher temperature than 320°C, polymerization maybe takes place. Here, we choose 320°C as annealing temperature). We then quickly cool the sample down to a specified temperature and measure the modulus. It has been shown that there are no solid crystals after annealing at high temperature for relative short periods due to supercooling behavior.<sup>1,25,26</sup>

The dynamic modulus of LC-5000 at different temperature are shown in Figure 6. The storage modulus

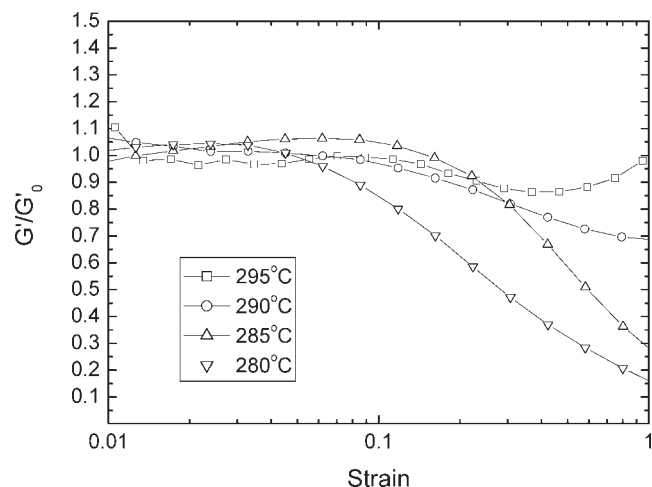


**Figure 5** Storage modulus versus strain for LC-5000 at different temperature.

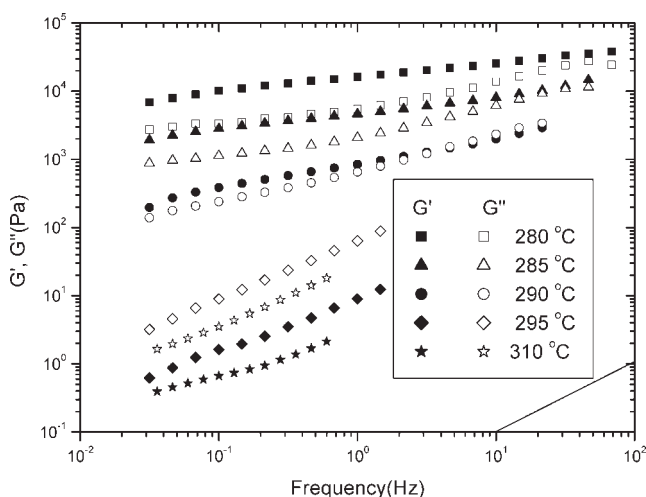


**Figure 6** Storage modulus ( $G'$ ) and loss modulus ( $G''$ ) versus frequency for LC-5000.

at 280, 285, and 290°C are larger than the loss modulus, which once again represents the behavior of a viscoelastic solid. The storage modulus becomes smaller than the loss modulus at 295 and 310°C, showing a behavior of viscoelastic liquid. Because of low viscosity at higher temperature,  $G'$  is not easily detected by the instrument. Rheological property at higher temperature is absent. The average content of solid crystals at different temperature can be extracted from Figure 6 by the Maron-Pierce equation, and the results are shown in Figure 7. The reduced solid content  $\phi/\phi_m$  decreases with the increase of temperature, and shows a sharp transition between 290 and 295°C. At 295°C, solid content is almost zero, which means complete melting of the solid crystals in nematic state. These results from dynamic frequency sweep are consistent with the  $\tan \delta$  curve in Figure 2.

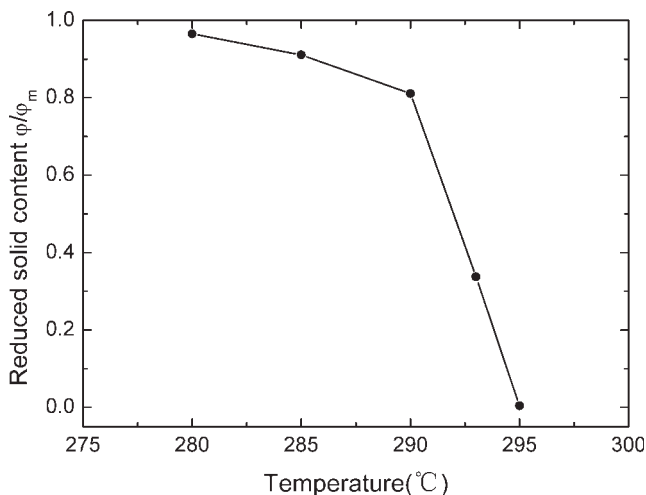


**Figure 7** Solid content of LC-5000 at different temperature.

## Relaxation behavior

It is seen from the dynamic modulus of LC-5000 (Fig. 6) that the slope of  $G'$  at low frequency is much smaller than 2, which implies that none of the samples shows the typical terminal behavior of entangled linear polymers. This means that there are certain slower relaxation processes that last beyond the scope of the dynamic experiments. Such long relaxation could possibly be detected by creep tests.<sup>27</sup> To show the long relaxation phenomena in dynamic modulus, we convert the creep compliance in Figure 4 first to a retardation spectrum, and then to the dynamic modulus by the nonlinear Tikhonov regularization method.<sup>28</sup> The combined dynamic modulus at 295°C is shown in Figure 8. The most interesting feature is the leveling off of  $G'$  toward low frequencies. Significant decrease of the slope of  $G'$  denotes a long relaxation mechanism. The relaxation spectrum  $H(\lambda)$  at 295°C is calculated from the combined dynamic modulus using the nonlinear Tikhonov regularization method<sup>28</sup> and the weighted spectrum  $\lambda H(\lambda)$  is shown in Figure 9. There are two characteristic peaks in the weighted spectrum, one at 50 s and the other larger than 2400 s. Generally, there are three kinds of relaxation mechanisms for nematic LCP: the relaxation of chain orientation, the relaxation of deformed polydomains, and the coalescence of polydomains (or the relaxation of textures). The relaxation of chain orientation without constraint is a much faster process, usually taking less than 2 s.<sup>17</sup> Such process is not seen in Figure 9 because of a lack of dynamic data at high frequency. The relaxation of deformed polydomains takes tens of seconds, which is reflected as the first peak in the weighted spectrum. The relaxation of texture is a very slow process, which requires thousands of

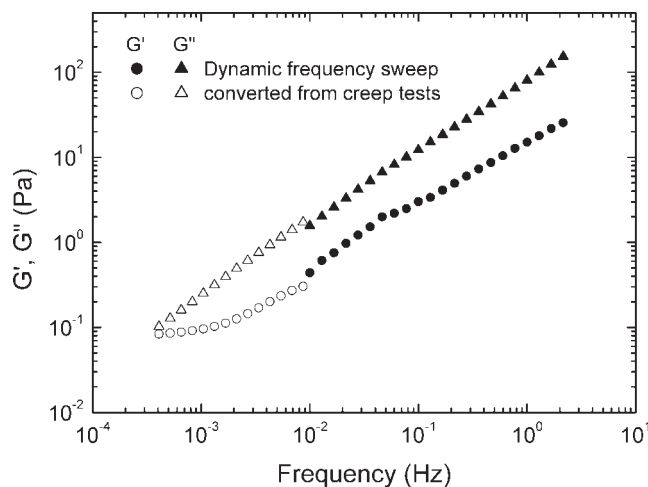


**Figure 8** The combined dynamic modulus of LC-5000 at 295°C.

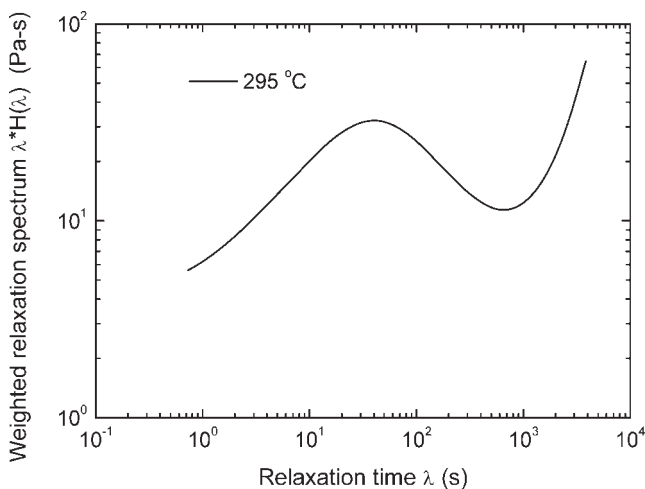


**Figure 9** The relaxation spectrum of LC-5000 at 295°C.

seconds. From the weighted relaxation spectrum, we surmise that the slow relaxation process corresponding to texture coarsening takes over 2400 s. The reason that the weighted relaxation spectrum does not show the long relaxation peak is that the creep test is not long enough (2400 s in present experiment).

This speculation has been verified by microscopic observations. Figure 10 shows a series of micrographs after the cessation of shear flow on LC-5000 at 295°C. At the beginning, the disclination lines are more or less aligned with the flow direction. We may consider these as delineating highly deformed and oriented domains. This picture is consistent with the observations of Geiger<sup>29</sup> that shear increases the number density and alignment of disclination loops. With the passing of time, their orientation of stretched disclination loops becomes more random. This relaxation occurs very fast in the first process; later the process becomes slower. The first period of fast relaxation is ascribed to retraction of stretched

polydomain, which corresponds to the characteristic time of 50 s in the weighted relaxation spectrum. The subsequent slow relaxation is attributed to coalescence of polydomains and hence the coarsening of the texture. We converted the POM images of LC-5000 at 295°C in Figure 10 into a power spectrum by discrete Fourier transform (DFT) to illustrate the textural length scale in real space.<sup>30</sup> A typical POM image and its power spectrum of two-dimensional DFT are shown in Figure 11. A distinct elongated shape at a certain orientation angle can be seen in the Figure 11. The deformation of the polydomain textures can be evaluated from the aspect ratio ( $b/a$ ) of its power spectrum. The aspect ratio  $b/a$  of polydomain is average of many domains, where  $b$  and  $a$  represent the axes length of stretched polydomain of its power spectrum. An ellipsoidal domain of TLCP gives rise to an ellipsoidal pattern in the power spectrum with the same aspect ratio but rotated by 90°. This result is shown in Figure 12, where the aspect ratios ( $b/a$ ) determined by spectrum is plotted against time. It can be seen that the aspect ratio of deformed texture decreases with time. It is apparent that there is a fast relaxation of the aspect ratio during the first 40 s, where a turning point appears, and a much slower process is followed. Here, the relaxation time determined by the aspect ratio ( $b/a$ ) of power spectrum by DFT is slightly shorter than the relaxation time (50 s) obtained from the relaxation time spectrum. This is because of a delay in starting the photography; the first picture in Figure 10 was in fact taken some 5–10 s after the step shear strain.

Such mechanism is appropriate for the relaxation of a TLCP in a fully nematic state. However, the situation changes if the sample contains solid crystals. The weighted relaxation spectra of LC-5000 at 280, 285, and 290°C are shown in Figure 13. A mild peak is seen below 10 s, and a second peak is expected

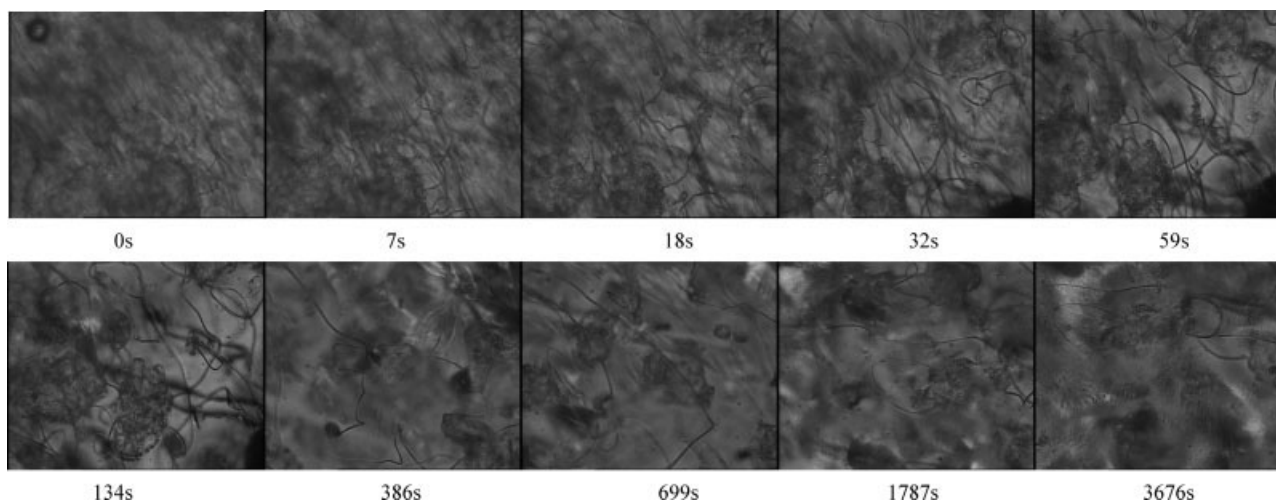


**Figure 10** Micrographs of LC-5000 after the cessation of shear flow at 295°C.

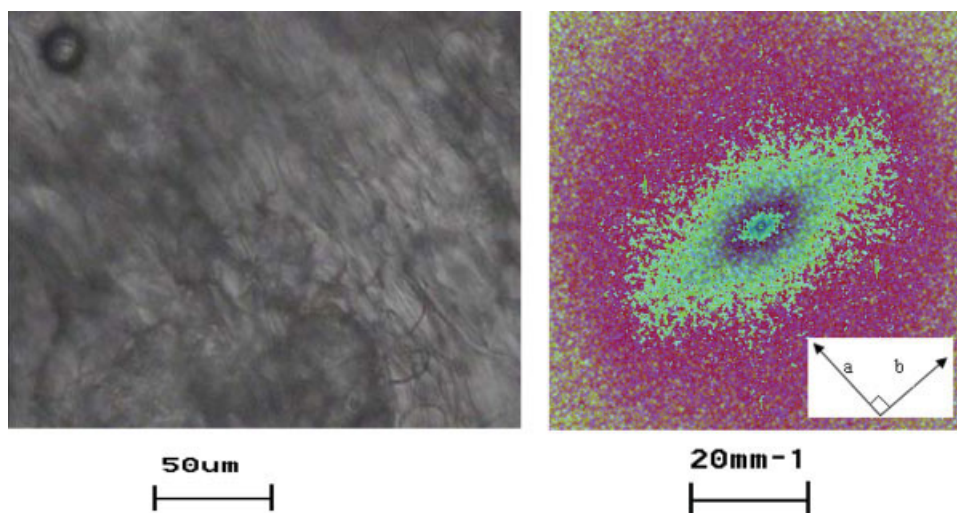


**Figure 11** A typical POM image and its power spectrum of two-dimensional DFT. [Color figure can be viewed in the online issue, which is available at [www.interscience.wiley.com](http://www.interscience.wiley.com).]

beyond 100 s. Moreover, the peak at time  $t < 10$  s shifts to shorter relaxation times as the temperature rises; it is different from the peak shown in Figure 9. A plausible explanation is that the peaks in Figure 13 for 280, 285, and 290°C reflect the relaxation of chain orientation. The retardance of the relaxation under relative low temperatures may be ascribed to two reasons. One is that the low temperature will decrease the motions of molecules. The other is that the TLCP is composed of nematic liquid crystal and residual solid crystals at 280, 285, and 290°C. The molecular chains and polydomains of nematic liquid crystal are restricted between residual solid crystals. The relaxation of chain orientation and deformed shape of polydomains under such constraining conditions should be slower than that without the constraints. Therefore, the relaxation time of orientation increases to about 3–5 s

at low temperature and that of deformed shape of polydomains increase to over 100 s. Both these relaxation times below 295°C are longer than those at 295°C, which correspond to a fully nematic state.

## CONCLUSIONS

The melting process of a thermotropic liquid-crystalline polymer LC-5000 is studied by DSC and dynamic temperature ramp. DSC analysis shows a wide melting interval, from 270 to 293°C, with a nominal melting point of 275°C. Rheological analyses via dynamic temperature ramp show transitions of the slope of  $G'$  and  $G''$  at about 294–295°C as well as a peak at 294°C in the loss tangent. The transition temperature detected by dynamic temperature ramp corresponds to the end of melting process.

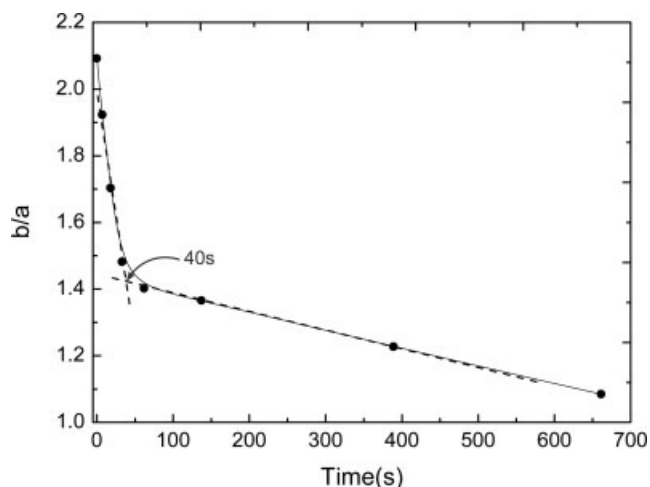


**Figure 12** The aspect ratio( $b/a$ ) of the deformed texture versus time.

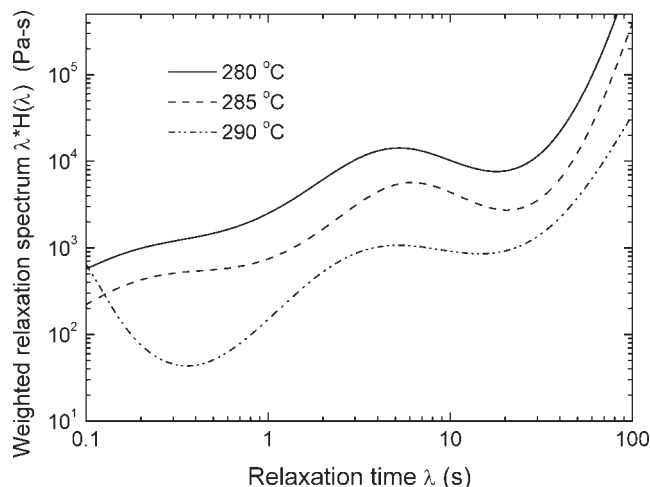


**Figure 13** The relaxation spectrum of LC-5000 at 280°C, 285°C and 290°C.

Further rheological experiments have been performed to verify the transition of LC-5000 from solid crystal to nematic state. The results of creep test, dynamic strain amplitude sweep, and dynamic frequency sweep show that LC-5000 is a viscoelastic solid between 270 and 294°C, and becomes a viscoelastic liquid at temperatures above 294°C. These results verify the idea that the sample is composed of a nematic liquid crystal and unmelted solid crystals. The contents of the solid crystals estimated from the loss modulus also show a sharp decrease between 290 and 295°C.

The relaxation behaviors of LC-5000 in the melting interval are greatly influenced by the solid crystals. The relaxation time of chain orientation and deformed polydomains under lower temperatures (<295°C) is longer than that at high temperatures (295°C), which is probably due to the constraints that the solid particles impose on the relaxation of the chains and polydomains of the nematic liquid crystal. Domain coalescence occurs after a much longer relaxation time (>2400 s).

## References

1. Driscoll, P.; Hayase, S.; Masuda, T. *Polym Eng Sci* 1994, 34, 519.
2. Wissbrun, K. F.; Griffin, A. C. *J Polym Sci: Polym Phys Ed* 1982, 20, 1835.
3. Kalika, D. S.; Giles, D. W.; Denn, M. M. *J Rheol* 1990, 34, 139.
4. Guskey, S. M.; Winter, H. H. *J Rheol* 1991, 35, 1191.
5. Cocchini, F.; Nobile, M. R.; Aciermo, D. *J Rheol* 1991, 35, 1171.
6. Han, C. D.; Kim, S. S. *J Rheol* 1994, 38, 13.
7. Han, C. D.; Kim, S. S. *J Rheol* 1994, 38, 31.
8. Wissbrun, K. F. *J Rheol* 1981, 25, 619.
9. Done, D.; Baird, D. G. *J Rheol* 1990, 34, 749.
10. Amundson, K. R.; Reimer, J. A.; Denn, M. M. *Macromolecules* 1991, 24, 3250.
11. Denn, M. M.; Reimer, J. A. In *Nematics: Mathematical and Physical Aspects*; Kluwer Academic: Boston, 1991; p 107.
12. Langelaan, H. C.; Gotsis, A. D. *J Rheol* 1996, 40, 107.
13. Beekmans, F.; Gotsis, A. D.; Norder, B. *J Rheol* 1996, 40, 947.
14. Moldenaers, P.; Mewis, J. *J Non-Newtonian Fluid Mech* 1990, 34, 359.
15. Burghardt, W. R.; Fuller, G. G. *Macromolecules* 1991, 24, 2546.
16. Lee, K. M.; Han, C. D. *Macromolecules* 2002, 35, 6263.
17. Wiberg, G.; Hillborg, H.; Gedde, U. W. *Polym Eng Sci* 1998, 38, 1278.
18. Donald, A. M.; Viney, G.; Windle, A. H. *Polymer* 1983, 24, 155.
19. Graziano, D. J.; Mackley, M. R. *Mol Cryst Liq Cryst* 1984, 106, 73.
20. Kwiatkowski, M.; Hinrichsen, G. *J Mater Sci* 1990, 28, 1550.
21. Tormes, M.; Munoz, M. E.; Pena, J. J.; Santamaria, A. *J Polym Sci, Part B: Polym Phys* 1998, 36, 253.
22. Gao, P.; Lu, X. H.; Chai, C.K. *Polym Eng Sci* 1996, 36, 2771.
23. Hsieh, T.; Tiu, C.; Simon, G. P. *J Appl Polym Sci* 2001, 82, 2252.
24. Poslinski, A. J. *J Rheol* 1988, 32, 703.
25. Done, D.; Baird, D. G. *Polym Eng Sci* 1990, 30, 989.
26. McLeod, M. A.; Baird, D. G. *J Appl Polym Sci* 1999, 73, 2209.
27. Kraft, M.; Meissner, J.; Kaschta, J. *Macromolecules* 1999, 32, 751.
28. Honerkamp, J.; Weese, J. *Continuum Mech Thermodyn* 1990, 2, 17.
29. Geiger, K. *Chem Eng Technol* 1998, 21, 157.
30. Hsiao, B. S.; Stenin, R.S.; Deutscher, K.; Winter, H. H. *J Polym Sci, Part B: Polym Phys* 1990, 28, 1571.